

Regulation of Chemokine Signal Integration by Activator of G-Protein Signaling 4 (AGS4)

William G. Robichaux III,¹ Melissa Branham-O'Connor,² Il-Young Hwang, Ali Vural,³ John H. Kehrl, and Joe B. Blumer

Department of Cell and Molecular Pharmacology and Experimental Therapeutics, Department of Neurosciences, Medical University of South Carolina, Charleston, South Carolina (W.G.R., M.B.-O., J.B.B.); and B-Cell Molecular Immunology Section, Laboratory of Immunoregulation, National Institute of Allergy and Infectious Diseases, National Institutes of Health, Bethesda, Maryland (I.-Y.H., A.V., J.H.K.)

Received October 23, 2016; accepted December 28, 2016

ABSTRACT

Activator of G-protein signaling 4 (AGS4)/G-protein signaling modulator 3 (Gpsm3) contains three G-protein regulatory (GPR) motifs, each of which can bind $G_{\alpha i}$ -GDP free of $G_{\beta\gamma}$. We previously demonstrated that the AGS4- $G_{\alpha i}$ interaction is regulated by seven transmembrane-spanning receptors (7-TMR), which may reflect direct coupling of the GPR- $G_{\alpha i}$ module to the receptor analogous to canonical $G_{\alpha\beta\gamma}$ heterotrimer. We have demonstrated that the AGS4- $G_{\alpha i}$ complex is regulated by chemokine receptors in an agonist-dependent manner that is receptor-proximal. As an initial approach to investigate the functional role(s) of this regulated interaction *in vivo*, we analyzed leukocytes, in which AGS4/Gpsm3 is predominantly expressed,

from AGS4/Gpsm3-null mice. Loss of AGS4/Gpsm3 resulted in mild but significant neutropenia and leukocytosis. Dendritic cells, T lymphocytes, and neutrophils from AGS4/Gpsm3-null mice also exhibited significant defects in chemoattractant-directed chemotaxis and extracellular signal-regulated kinase activation. An *in vivo* peritonitis model revealed a dramatic reduction in the ability of AGS4/Gpsm3-null neutrophils to migrate to primary sites of inflammation. Taken together, these data suggest that AGS4/Gpsm3 is required for proper chemokine signal processing in leukocytes and provide further evidence for the importance of the GPR- $G_{\alpha i}$ module in the regulation of leukocyte function.

Introduction

Signal processing in response to chemoattractant-stimulated activation of cognate seven transmembrane-span receptors (7-TMRs) is a key event in regulating leukocyte behavior.

This work was supported by the National Institutes of Health (NIH) National Institute of General Medical Sciences [Grant R01-GM086510 to J.B.B.], National Institute of General Medical Sciences South Carolina Institutional Development Awards Networks of Biomedical Research Excellence [Grant P20-GM103499 to M.B.O.], National Cancer Institute [Grant T32-CA119945 to M.B.O.], MUSC institutional funds (to J.B.B.), and the intramural research program of the National Institute of Allergy and Infectious Diseases (to J.H.K.). This work was also enabled by support from the National Institutes of Health National Institute on Neurological Disorders and Stroke [Grant R01-NS24821] and National Institute on Drug Abuse [Grant R01-DA025896], both to Dr. Stephen M. Lanier (Wayne State University). The research presented in this article was supported in part by the Flow Cytometry and Cell Sorting Shared Resource, funded by a Cancer Center Support grant from the National Cancer Institute [Grant P30 CA138313 to the Hollings Cancer Center at the Medical University of South Carolina] and in part by the National Center for Research Resources and the Office of the Director of the National Institutes of Health [Grant C06 RR015455 to the Hollings Cancer Center at the Medical University of South Carolina].

¹Current affiliation: University of Texas Health Science Center, Houston, Houston, Texas.

²Current affiliation: Department of Biology, Charleston Southern University.

³Current affiliation: Department of Pharmacology, Wayne State University, Detroit, Michigan.

dx.doi.org/10.1124/jpet.116.238436.

Effective signal integration in leukocytes requires appropriate regulation of signal transfer from receptor to G protein and G protein to effector to allow cells to process and prioritize incoming signals and provide flexibility to adapt to a changing environment. Leukocyte migration and functional capacity as part of the immune response is tightly regulated by chemokines and other chemoattractants, which signal via $G_{\alpha i}$ -coupled GPCRs. $G_{\alpha i}$ in particular plays critical roles in regulating leukocyte migration and response to infection (e.g., Pero et al., 2007; Zarbock et al., 2007; Wiege et al., 2013). The mechanisms regulating chemokine and chemoattractant-stimulated responses of leukocytes are keys to understanding signal processing during inflammation and immune challenge, and the identification and characterization of entities that modulate leukocyte responsiveness are of great interest and importance to the field as well as providing novel targets for potential therapeutic manipulation.

Accessory proteins for heterotrimeric G-protein signaling systems play integral roles in processing signals emanating from cell-surface 7TM receptors. One family of accessory proteins includes the group II activator of G-protein signaling

ABBREVIATIONS: 7-TMR, seven-transmembrane receptor; AGS, activator of G-protein signaling; BRET, bioluminescence resonance energy transfer; BSA, bovine serum albumin; DC, dendritic cell; DPBS, Dulbecco's phosphate-buffered saline; ERK, extracellular signal-regulated kinase; FITC, fluorescein isothiocyanate; fMLP, N-formyl-methionine-leucine-phenylalanine; Gnai, guanine nucleotide-binding protein G(i), α subunit; GPCR, G-protein coupled receptor; GPR, G-protein regulatory; Gpsm, G-protein signaling modulator; HEK293, human embryonic kidney cell line 293; KOMP, Knockout Mouse Project; PBS, phosphate-buffered saline; PTX, pertussis toxin; RGS, regulator of G-protein signaling; TBST, Tris-buffered saline + 0.01% Tween; WT, wild-type; YFP, yellow fluorescent protein.

(AGS) proteins, which were identified in a yeast-based functional screen for entities that activated heterotrimeric G-proteins in the absence of a cell-surface receptor (Cismowski et al., 1999; Takesono et al., 1999). Group II AGS proteins, including AGS3/G-protein signaling modulator 1 (Gpsm1) and AGS4/Gpsm3, are characterized by the presence of at least one G-protein regulatory (GPR) motif, which bind G α i-GDP in the absence of G $\beta\gamma$.

Group II AGS proteins have shown a surprising diversity of regulatory functions. AGS3 is involved in a number of biological functions in addition to asymmetric cell division, including addiction (Bowers et al., 2004, 2008; Yao et al., 2005, 2006), polycystic kidney disease and response to renal ischemia reperfusion injury (Nadella et al., 2010; Regner et al., 2011; Kwon et al., 2012), cardiovascular regulation (Blumer et al., 2008; Chauhan et al., 2012), lysosomal biogenesis and bacterial infection (Vural et al., 2016), and chemokine signal processing (including leukocyte chemotaxis) (Kamakura et al., 2013; Branham-O'Connor et al., 2014; Singh et al., 2014). The immune system in particular requires dynamic signal processing and spatially integrated G-protein signaling, including the use of accessory proteins (e.g., Moratz et al., 2000, 2004; Han et al., 2005, 2006; Hwang et al., 2013; Boularan and Kehrl, 2014; Branham-O'Connor et al., 2014; Huang et al., 2014; Boularan et al., 2015; Hwang et al., 2015). AGS4 [gene name: G-protein signaling modulator 3 (Gpsm3)] contains three GPR motifs and is of particular interest for its predominant expression in the immune system (Giguère et al., 2013, *vide infra*), where its expression appears to be responsive to external stimuli (Cho, H., Kehrl, J.H., and Blumer, J.B., unpublished observations) and has been linked to autoimmune and inflammatory diseases (Nakou et al., 2008; Ahn et al., 2012; Kiliszek et al., 2012; Yan et al., 2012; Zhong et al., 2012; Kupfer et al., 2013; Billard et al., 2014; Giguère et al., 2014; Gall et al., 2016).

We previously demonstrated that the G α i-AGS4/Gpsm3 interaction is regulated by a cell-surface 7-TMR (Oner et al., 2010b; Robichaux et al., 2015), thus providing an alternative mode of input to heterotrimeric G proteins, which may complement and/or extend canonical receptor—G-protein—effector signaling systems; however, regulation of G α i-AGS4 complex by chemokine receptors and the functional consequence of such regulation and its impact on chemokine-regulated G-protein signal processing is unknown. As part of an expanded approach to define the functional roles of AGS4/Gpsm3 *in vivo*, we used AGS4/Gpsm3-null mice, with an initial investigation into the role of AGS4 in chemoattractant signal processing. Our data indicate that AGS4/Gpsm3 plays an important role in processing signals emanating from chemoattractant receptors that regulate leukocyte motility, thus further expanding the functional roles of G-protein signal modulators in the immune system.

Materials and Methods

Materials. Pertussis toxin, β -actin antibody (A5441), lipopolysaccharides from *Escherichia coli* 0111:B4 (L4391), N-Formyl-Met-Leu-Phe (fMLP) (F3506), AMD3100 (plerixafor), and thioglycollate broth (USP Alternative, 70157) were purchased from Sigma-Aldrich (St. Louis, MO). Recombinant mouse GM-CSF, CXCL12, and CCL19 were obtained from BioAbChem Inc. (Ladson, SC). AGS4 antibody (AP5725c), anti-phospho-extracellular signal-regulated kinase (ERK) (Tyr⁴⁰²), and total ERK were purchased from Abgent (San

Diego, CA), Santa Cruz Biotechnology (Dallas, TX), and Abcam (Cambridge, MA), respectively. Protease inhibitor cocktail tablets (Complete Mini) were obtained from Roche Life Science (Indianapolis, IN). ACK Lysing Buffer (0.15 M NH₄Cl/0.01M KHCO₃/10 μ M EDTA, 10-548E) was obtained from Lonza (Basel, Switzerland) and Percoll (17-089-02) from GE Healthcare Life Sciences (Pittsburgh, PA). Dynabeads Untouched Mouse T Cells kit (11413D) was purchased from Invitrogen Life Technologies (Grand Island, NY). Corning HTS Transwell 96-well plates (09-761-83) as well as other materials and media for cell culture were obtained from Fisher Scientific (Waltham, MA). Conjugated antibodies fluorescein isothiocyanate (FITC)-CD11b (557396), isotype FITC-rat IgG2a, κ (553929), PE-Ly-6G (551461), and isotype PE-Rat IgG2b, κ (553989) were purchased from BD Biosciences (San Jose, CA). pcDNA3::CXCR4 and pIRES-puro-CXCR4-Venus were kind gifts from Dr. Michel Bouvier (University of Montreal, Montreal, QC, Canada) (Hamdan et al., 2006). Other materials were obtained as described elsewhere (Oner et al., 2010a, 2010b, 2013; Branham-O'Connor et al., 2014; Robichaux et al., 2015).

Bioluminescence Resonance Energy Transfer. Bioluminescence resonance energy transfer (BRET) experiments were performed in human embryonic kidney line 293 (HEK293) cells as previously described (Oner et al., 2010b; 2013). Briefly, 1×10^6 cells were plated per well in a six-well plate the day before transfection with 2 ng of pHRLucN3::AGS4 or AGS4-Q/A and 500 ng pcDNA3::G α i2-yellow fluorescent protein (YFP), 500 ng pcDNA3.1::CXCR4, 750 ng pIRES-puro-CXCR4-Venus and/or 750 ng pcDNA3::G α i2 as indicated in the figure or figure legend using polyethylenimine as described (Oner et al., 2010b, 2013). Empty pcDNA3 was used to bring the total amount of DNA used per transfection to 1.5 μ g. Forty-eight hours after cell transfection, cells were dispensed in triplicate at 1×10^5 cells/well in gray 96-well Optiplates (PerkinElmer, Waltham, MA). Fluorescence and luminescence signals were measured using a TriStar LB 941 plate reader (Berthold Technologies USA, Oak Ridge, TN) with MikroWin 2000 software (Mikrotek, Overath, Germany). Cells were incubated with the CXCR4 agonist CXCL12 (10 μ M) or vehicle (Tyrode solution: 140 mM NaCl, 5 mM KCl, 1 mM MgCl₂, 1 mM CaCl₂, 0.37 mM NaH₂PO₄, 24 mM NaHCO₃, 10 mM HEPES, pH 7.4, and 0.1% glucose (w/v)) for 5 minutes before the addition of coelenterazine H. Coelenterazine H (5- μ M final concentration; Nanolight Technology, Pinetop, AZ) was added to each well, and luminescence was measured after 2 minutes (donor: 480 + 20 nm; acceptor: 530 + 20 nm) with the TriStar LB 941 plate reader. BRET signals were determined by calculating the ratio of the light intensity emitted by the YFP divided by the light intensity emitted by RLuc. Net BRET values were determined by first calculating the $530 \pm 20:480 \pm 20$ nm ratio and then subtracting the background BRET signal determined from cells transfected with the donor plasmid pHRLucN3::AGS4 alone.

Mouse Models. Gpsm3^{-/-} mice generated in the C57BL/6 background were obtained through the Knockout Mouse Project (KOMP) consortium (strain Gpsm3^{tm1(KOMP)Wtsi}; <http://www.mousephenotype.org/data/alleles/MGI:2146785/tm1%28KOMP%29Wtsi>). Details on the targeting vector can be found at https://www.i-dcc.org/imits/targ_rep/alleles/12506/vector-image. Briefly, 5' and 3' homology arms (6260 bp comprising exon 1 of Gpsm3 and surrounding regions and 4155 bp, consisting of Gpsm3 exon 4 and surrounding regions, respectively) flanking a floxed neomycin-resistance cassette, and promoterless lacZ was inserted into genomic Gpsm3 by homologous recombination. Genotyping of mice was performed with a three-primer polymerase chain reaction design using a forward primer from the 5' end of the first exon of Gpsm3 (mgGpsm3 16651 forward), a second forward primer that is specific to the targeting plasmid (common 3' forward), and a reverse primer from Gpsm3 exon 4 of the Gpsm3 coding sequence (CSD-Gpsm3-SR1). The primer sequences are as follows: mgGpsm3 16651 forward primer 5'-TGA CGG GTG GAC ACA GGA GAC TTG GGA AAG-3' Common 3' forward (universal RAF5 forward) 5'-CAC ACC TCC CCC TGA ACC TGA AA-3'; CSD-Gpsm3-SR1 5'-CAG GGA AAG TGG GTG GTA AAT ACA G-3'. Using this strategy, a 1200-bp band representing wild-type

Gpsm3 would result from priming from mgGpsm3 16651 forward and CSD-Gpsm3-SR1 and a 776-bp band representing the Gpsm3-null allele would result from priming common 3 forward and CSD-Gpsm3-SR1 (Fig. 2A). Wild-type and Gpsm3^{-/-} female littermates at 6–12 weeks of age generated from Gpsm3^{+/-} intercrosses were used. Tissues and lysates were prepared and processed for immunoblotting as described (Blumer et al., 2002) and as described below in the *Immunoblotting* section of this article.

Complete Blood Count Analysis. Cardiac puncture was administered to euthanized wild-type (WT) or Gpsm3^{-/-} mice using 1 ml of syringe fitted with a 21-gauge needle to harvest fresh blood from the left ventricle, slowly to prevent cardiac collapse of the heart, and subsequently blood was collected in BD Microtainer tubes (BD Biosciences, Franklin Lakes, NJ) containing EDTA. Samples were maintained at constant temperature and humidity throughout processing and analysis. Complete blood cell counts were performed using a HemaVet 950 (Drew Scientific, Dallas, TX) instrument to measure leukocyte, erythrocyte, and thrombocyte levels in each sample. Machine calibration and performance were verified each day that samples were analyzed using MULTI-TROL standard solution (Dog, Drew Scientific). All samples were run within 2 hours of initial collection.

Primary Cells. To isolate dendritic cells, bone marrow was isolated from WT or Gpsm3^{-/-} mouse femurs and tibiae using a 25-gauge syringe to flush the bone marrow out with 10 ml of DPBS [Dulbecco's phosphate-buffered saline (PBS), Ca⁺⁺, and Mg⁺⁺ free]. Isolated bone marrow was then filtered through a 40- μ m nylon cell strainer, centrifuged at 4°C 500g, and decanted. Red blood cells were lysed with 5 ml of ice-cold ACK lysis buffer (0.17 M NH₄Cl/0.17 M Tris) for 5 minutes at room temperature, followed by an additional spin at 4°C 500g to pellet the harvested bone marrow cells. Isolated cells were then resuspended in 10 ml of dendritic cell (DC) I media (RPMI-1640 supplemented with 10% fetal bovine serum, 100 U/ml penicillin, 100 mg/ml streptomycin, and 20 ng/ml rmGM-CSF), and plated 4 or 5 \times 10⁵ cells/ml in a 10-cm tissue culture dish. On day 4, 10 ml of fresh DC I media was added to each dish. On day 8, nonadherent and loosely adherent cells were harvested, centrifuged 4°C 500g, decanted, and reseeded in 10 ml of fresh DC II media (RPMI-1640 supplemented with 10% fetal bovine serum, 100 U/ml penicillin, 100 mg/ml streptomycin, and 10 ng/ml rmGM-CSF) to generate immature dendritic cells. Day 9 cells were treated with or without 200 ng/ml lipopolysaccharide for the indicated times or for 24 hours to generate mature DCs. To isolate splenic B- and T-lymphocytes, spleens of WT or Gpsm3^{-/-} mice were gently crushed between frosted glass slides in 10 ml of serum-free RPMI. Spleen homogenate was centrifuged at 4°C 500g and decanted. Red blood cells were lysed with 10 ml of ice-cold ACK lysing buffer for 5 minutes at room temperature, followed by an additional spin at 4°C 500g to pellet the splenocytes. Splenocytes were then washed once and resuspended in DPBS supplemented with 0.1% bovine serum albumin (BSA) and 2 mM EDTA at 5 \times 10⁷ cells/ml or 1 \times 10⁸ cells/ml for subsequent B- or T-cell isolation, respectively. Cell isolation was performed according to the Invitrogen Dynabeads protocol for untouched B-cell isolation or negative T-cell isolation. For neutrophil isolation, bone marrow was isolated from WT or Gpsm3^{-/-} mouse femurs and tibiae using a 25-gauge syringe to flush the bone marrow with 10 ml of DPBS. Isolated bone marrow was then filtered through a 40- μ m nylon cell strainer, centrifuged at 4°C at 500g, and decanted. Pelleted cells were resuspended in 2 ml of DPBS, followed by subsequent careful layering on top a three-layer Percoll density gradient. The density gradient was generated by diluting 100% Percoll in DPBS to the required densities represented by 78%, 64%, and 52% Percoll dilutions. Stacking of the different layers was conducted as follows: 3 ml of 78% Percoll, 2 ml of 64% Percoll, and 2 ml 52% Percoll, followed by subsequent 2 ml of sample. After centrifugation at 1500g for 40 minutes at 4°C, the 78%/64% Percoll interface was carefully isolated and added to 9 ml of DPBS to disrupt the remaining gradient. Isolated cells were then centrifuged 4°C, 1500g for 5 minutes, decanted, and subjected to 1 ml of ice-cold ACK lysis buffer for

5 minutes at room temperature to remove any remaining red blood cells. Cells were then resuspended in 1 or 2 ml of phenol red-free RPMI supplemented with 0.1% BSA and 2 mM EDTA.

Immunoblotting. Single-cell suspensions from spleen were prepared by crushing freshly dissected tissues between frosted glass slides in 10 mL DPBS. After centrifugation at 4°C 500g for 5 minutes, samples were decanted and red blood cells were lysed with 10 ml of ice-cold ACK lysis buffer for 5 minutes at room temperature, followed by a second round of centrifugation at 4°C 500g for 5 minutes. ACK lysis buffer was then decanted and pellets were resuspended in 100–300 μ l of 1% NP40 lysis buffer (50 mM Tris, pH 8.0, 150 mM NaCl, 5 mM EDTA, 1% Nonidet P-40) with protease inhibitors. Samples were incubated on ice for 20 minutes followed by centrifugation at 10,000g for 30 minutes at 4°C. Primary cultures of dendritic cells were harvested using cell scrapers, and neutrophils were collected after Percoll density centrifugation to be processed in 1% NP-40 lysis buffer with protease inhibitors as described above. Protein concentration was determined by Pierce BCA protein assay (Thermo Scientific, Waltham, MA). Protein samples were subjected to SDS-PAGE, 10%–13.5% and separated proteins were transferred to polyvinylidene difluoride membranes for immunoblotting as described (Blumer et al., 2002). Immunoblotting with AGS4 antibodies (Abgent, San Diego, CA) was conducted as follows: Membranes were then blocked with 50% Odyssey Buffer [LI-COR Biosciences] and 50% Tris-buffered saline + 0.01% Tween (TBST) for 30 minutes at room temperature, incubated with AGS4 antibody (1:250 dilution) overnight at 4°C, followed by three 10-minute washes in TBST. Membranes were then exposed to 1:5000 dilution of horseradish peroxidase-conjugated goat anti-rabbit IgG for 30 minutes at room temperature, followed by three 30-minute washes with TBST and subsequent exposure with ECL.

Phospho-ERK (pERK) Assays. Single-cell suspensions of WT and Gpsm3^{-/-} cultured dendritic cells or freshly isolated splenocytes were isolated as described. Cells were stimulated in the absence or presence of 200 ng/ml CXCL12, a concentration based on our previous experience with primary dendritic cell cultures and splenocytes (Branham-O'Connor et al., 2014) and that of others (Basu and Broxmeyer, 2005, 2009; Petit et al., 2005; Dorner et al., 2009; Boudot et al., 2014), for 0.5, 2, and 5 minutes. At the indicated times, cells were immediately lysed in 1% NP40 buffer with protease inhibitors and additional phosphatase inhibitors (50 mM NaF, 5 mM sodium pyrophosphate, 40 mM β -glycerophosphate, and 200 μ M Na₃VO₄) on ice for 20 minutes followed by centrifugation at 10,000g for 30 minutes at 4°C. Samples were subjected to SDS-PAGE, and proteins were transferred to polyvinylidene difluoride membranes and immunoblotted for anti-phospho-Erk (Y402) (Santa Cruz Biotechnology, Dallas, TX) or total Erk (Abcam) antibodies. Densitometric quantification of the immunoblotted bands was performed using ImageJ densitometry software (Version 1.49i, National Institutes of Health, Bethesda, MD). Selected bands were quantified based on their relative intensities and normalized to total Erk.

Chemotaxis. Corning Transwell 24-well inserts (6.5-mm diameter, 5.0- μ m pore size) or 96-well inserts (5.0- μ m pore size) were used for all chemotaxis assays. For dendritic cell chemotaxis, 235 μ l of serum-free RPMI with or without CXCL12 (10–500 ng/ml) or CCL19 (250 ng/ml) was added to each lower chamber and 75 μ l of approximately 3 \times 10⁶ cells/ml were loaded into the upper chambers. For T-lymphocytes, 235 μ l of serum-free RPMI supplemented with 0.1% BSA and 2 mM EDTA with or without CCL19 (50–300 ng/ml) was added to each lower chamber, and 75 μ l of approximately 1 \times 10⁷ lymphocytes/mL were added into the upper chambers. For neutrophils, 235 μ l of serum-free RPMI supplemented with 0.1% BSA and 2 mM EDTA with or without fMLP (0.1–5.0 μ M) was added to each lower chamber, and 75 μ l of approximately 5 \times 10⁶ cells/ml were added to the upper chambers. Chemotaxis chambers were incubated at 37°C, 5% CO₂ for 20 hours for dendritic cells, 5 hours for lymphocytes, and 3 hours for neutrophils. The upper chamber was removed, and cells migrating to the bottom chamber as well as cells retained in the upper chamber were counted by flow cytometry.

The percentage of cells that migrated was calculated relative to the input, where the number of cells migrating to the bottom chamber in the absence of chemokine was subtracted. Chemotaxis data shown are the means \pm S.E. from at least three independent experiments, each containing at least triplicate determinations.

Thioglycollate-Induced Intraperitoneal Inflammation. WT and *Gpsm3*^{-/-} mice received i.p. injections using an insulin syringe (28-gauge) to deliver 1 ml of DPBS or 4% thioglycollate (in DPBS, sterilized, and aged for a minimum of 2 weeks). After 2 hours, mice were euthanized and i.p. cavity lavage was carried out through injection of 10 ml of cold DPBS and thorough subsequent agitation of the cavity. Blood (350–600 μ l) was also collected by cardiac puncture and bone marrow was collected from femurs as described above in the *Primary Cells* section of this article. Isolated cells were centrifuged at 4°C 500g for 5 minutes, with excess supernatant decanted, and red blood cells were lysed using 1 ml of ice-cold ACK lysis buffer (5-minute incubation followed by subsequent 500 \times g centrifugation for 5 minutes). Blood samples required a minimum of two ACK lysis steps to remove all of the red blood cells. Isolated i.p. lavage cells were then resuspended in 50 μ l of PBS with 1% BSA and 0.1% NaN₃ (PBS-BSA), isolated cells from the blood were resuspended in 200 μ l of PBS-BSA, and isolated bone marrow cells were resuspended in 1 ml of PBS-BSA. Each sample then had 50 μ l subjected to incubation with conjugated antibodies for analysis by flow cytometry, described as follows.

Flow Cytometry and Cell Sorting. Single-cell suspensions of WT and *Gpsm3*^{-/-} neutrophils collected from Percoll density centrifugation or from thioglycollate-induced inflammation experiments were prepared as described. Cell pellets were washed and resuspended in 50 μ l of PBS supplemented with 1% BSA and 0.1% NaN₃ (PBS-BSA). Cells were incubated with primary fluorescein isothiocyanate FITC-CD11b (0.3 μ l, 0.15 μ g) or PE-Ly-6G (2 μ l, 0.4 μ g) conjugated antibodies or isotype controls FITC-rat IgG2a, κ (1 μ l, 0.5 μ g), or PE-Rat IgG2b, κ (3 μ l, 0.6 μ g) in PBS-BSA for 30 minutes at 4°C (BD Pharmingen, San Diego, CA). Cells were washed thrice with 500 μ l PBS-BSA with subsequent centrifugations at 4°C 500g 5 minutes, and resuspended in 250–500 μ l of PBS-BSA for analysis by flow cytometer (BD Pharmingen). Neutrophil populations were observed as being dual positive (CD11b⁺, Ly-6G⁺).

Data Analysis. Statistical significance for differences involving a single intervention was determined by one-way analysis of variance, followed by a post hoc Tukey's test using GraphPad Prism version 4.03 (GraphPad Software, San Diego).

Results

We previously demonstrated that the *Gai*-AGS4 interaction is regulated by *Gai*-coupled 7-TM receptors such as the α_2 -adrenergic receptor (Oner et al., 2010b; Robichaux et al., 2015). As an initial approach to determine whether such regulation of *Gai*-AGS4 extends to chemokine receptors, which are widely expressed in the immune system and are *Gai*-coupled, we used our previously established bioluminescence resonance energy transfer (BRET) platform to monitor the *Gai*-AGS4 interaction in real-time in live cells (HEK293) in response to the expression and activation of a prototypical chemokine receptor, CXCR4. Activation of CXCR4 by the agonist CXCL12 significantly reduced the *Gai*₂-AGS4 interaction, indicating that regulation of this complex is indeed sensitive to chemokine receptor activation (Fig. 1A). CXCL12 regulation of the *Gai*₂-AGS4 complex required the presence of CXCR4 and was blocked by the CXCR4 antagonist AMD3100 (plerixafor) and by pertussis toxin pretreatment, which ADP-ribosylates *Gai* and prevents receptor and G-protein coupling. BRET signals were completely absent with a mutant form of AGS4 in which a conserved glutamate residue in each of its

three GPR motifs was mutated to alanine (AGS4-Q/A), rendering it incapable of binding *Gai* (Cao et al., 2004; Oner et al., 2010b), which serves as an internal negative control for the system (Fig. 1A).

We next sought to determine whether AGS4-*Gai* complexes might actually interface directly with CXCR4 in an agonist-regulated manner by modifying our BRET platform to include CXCR4-Venus as the acceptor rather than *Gai*₂-YFP (Fig. 1B, top panel). In the absence of coexpressed *Gai*₂, AGS4-CXCR4 BRET signals were only slightly above background; however, when *Gai*₂ was coexpressed, a robust AGS4-CXCR4 BRET signal was observed, indicating a *Gai*₂-dependent tripartite complex between AGS4, *Gai*₂, and CXCR4 (Fig. 1B, bottom panel). This complex was also regulated by CXCL12, the effect of which was blocked by the antagonist AMD3100 (plerixafor) and pertussis toxin pretreatment (Fig. 1B). Taken together, these data are consistent with our previous data (Oner et al., 2010b; Robichaux et al., 2015) and indicate that the AGS4-*Gai* module is capable of forming a complex with CXCR4 that is agonist-dependent, with broad implications on chemokine signal integration.

To further understand the functional consequence of this novel regulation and as part of an ongoing effort to define the functional roles of GPR proteins in the immune system (e.g., Branham-O'Connor et al., 2014), AGS4/*Gpsm3*-null mice were used (see *Materials and Methods* for details). Genotyping and immunoblotting confirmed that the insertion of the targeting plasmid resulted in the loss of AGS4 protein expression (Fig. 2, A and B).

The location of the *Gpsm3* gene within the class III major histocompatibility class locus suggested that AGS4/*Gpsm3* is expressed primarily in the immune system, and initial observations from us and others indicated this was indeed the case (Cao et al., 2004; Kimple et al., 2004; Zhao et al., 2010; Schmidt et al., 2012; Giguère et al., 2013). We also discovered AGS4 expression in primary bone marrow-derived dendritic cells and splenocytes (Fig. 2B). Complete blood count analysis indicated that AGS4/*Gpsm3*-null mice exhibited a mild but significant neutropenia and lymphocytosis, whereas other leukocyte populations were unaltered (Fig. 2C).

As an initial approach to determine the role of AGS4 in G-protein signal processing in leukocytes, we examined the chemokine-mediated activation of ERK1/2 in primary dendritic cells and splenocytes. Loss of AGS4/*Gpsm3* expression resulted in a reduction in CXCL12-activated ERK1/2 phosphorylation in both populations of cells (Fig. 3), suggesting a role for AGS4 in chemokine signal processing. In conjunction with the known role of *Gai*-based signaling in chemotaxis (e.g., Rudolph et al., 1995; Han et al., 2005; Hwang et al., 2007; Zarbock et al., 2007; Cho et al., 2012; Wiege et al., 2012; Surve et al., 2016), previous reports also indicate that ERK1/2 activation subsequent to chemokine receptor stimulation plays an important role in directed migration of leukocytes (Tilton et al., 2000; Delgado-Martín et al., 2011; Sagar et al., 2012). To explore the possible role of AGS4/*Gpsm3* in chemotaxis, we measured chemokine-directed migration in primary dendritic cells and T lymphocytes. We observed ~25% reductions in CXCL12-directed chemotaxis in primary dendritic cells and CCL19-directed chemotaxis in primary T lymphocytes from AGS4/*Gpsm3*-null mice compared with WT mice (Fig. 4, A and B). No significant differences were found in the random migration of primary dendritic cells and T lymphocytes from AGS4/*Gpsm3*-null and WT mice, indicating

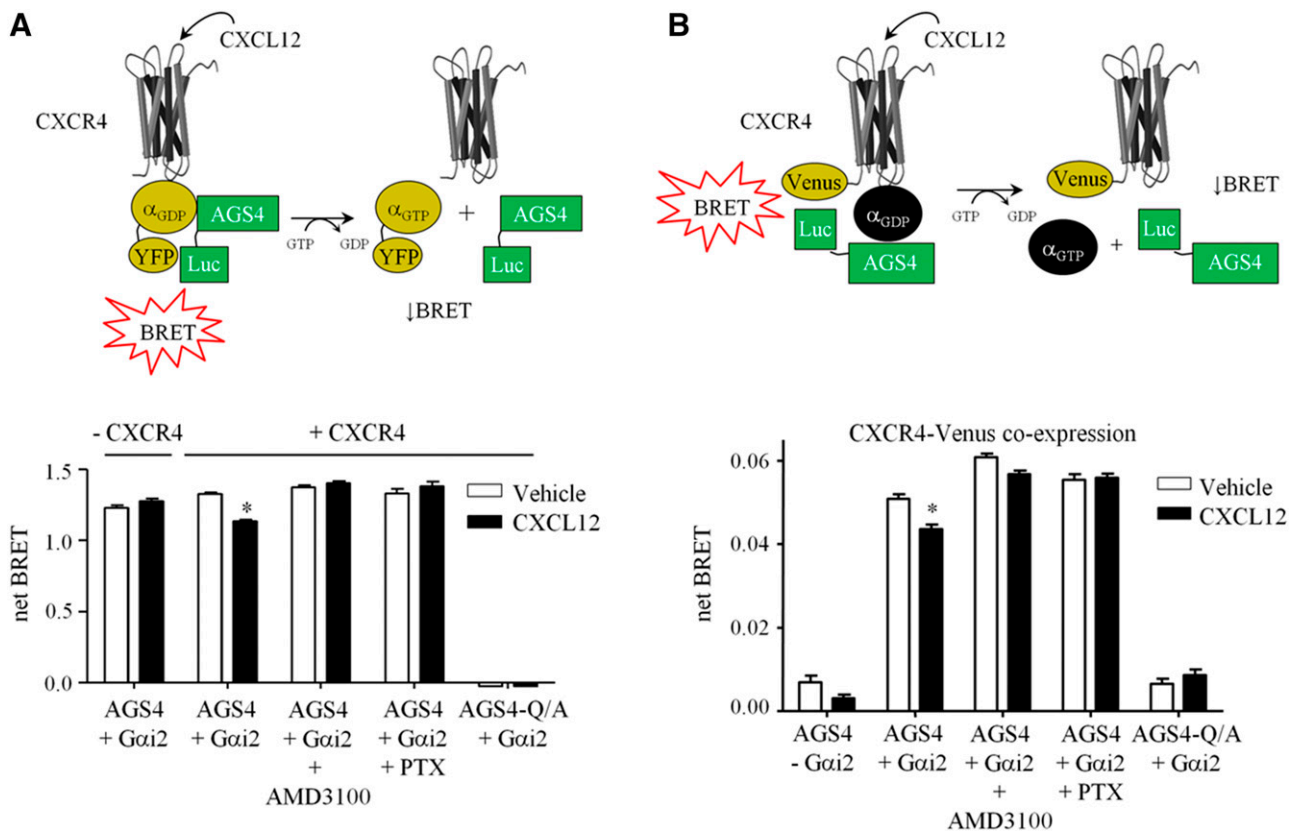


Fig. 1. Regulation of Gai_2 -AGS4 interaction by the prototype chemokine receptor CXCR4. (A) Top panel: Schematic of BRET system along with representation of hypothesized agonist-induced regulation of Gai_2 YFP/AGS4-Rluc BRET association by receptor activation. For simplification, AGS4-Rluc is shown interacting with a single Gai_2 -YFP; however, AGS4 can bind multiple Gai subunits simultaneously (Kimple et al., 2004; Oner et al., 2010b), which may be responsible for the robust BRET signals observed (Oner et al., 2010b). Bottom panel: Net BRET signals were obtained from HEK293 cells transfected with 2 ng of phRLuc_{N3}::AGS4 or 2 ng of phRLuc_{N3}::AGS4-Q/A-Rluc and 500 ng of pcDNA3:: Gai_2 -YFP. Cells were also transfected in the presence or absence of 500 ng pcDNA3::CXCR4. Vehicle (Tyrode's solution) or CXCL12 (100 ng/ml) were added to cells as indicated, followed by fluorescence and luminescence readings as described in *Materials and Methods*. The CXCR4 antagonist AMD3100 (plerixafor, 1 μ g/ml) was added 10 minutes before agonist stimulation as indicated. Cells were treated with pertussis toxin (PTX, 100 ng/ml) 18 hours before receptor stimulation where indicated. Data are expressed as means \pm S.E.M. from three independent experiments with triplicate determinations ($n = 9$). * $P < 0.0001$ as compared with vehicle-treated control group as determined by one-way analysis of variance with Tukey's post-hoc test. (B) Top panel: Schematic representing the BRET system used to measure effect of chemokine receptor activation on the proximity of Gai -AGS4 complex to CXCR4-Venus. Bottom panel: HEK cells were transfected with 2 ng of phRLuc_{N3}::AGS4 or 2 ng phRLuc_{N3}::AGS4-Q/A along with 750 ng pIRESpuro3::CXCR4-Venus in the presence or absence of 750 ng pcDNA3:: Gai_2 as indicated. Vehicle (Tyrode's solution) or CXCL12 (100 ng/ml) was added to cells as indicated, followed by fluorescence and luminescence readings as described in *Materials and Methods*. The CXCR4 antagonist AMD3100 (plerixafor, 1 μ g/ml) was added 10 minutes before agonist stimulation as indicated. Cells were treated with pertussis toxin (PTX, 100 ng/ml) 18 hours before receptor stimulation where indicated. Data are expressed as means \pm S.E.M. from at least three independent experiments with triplicate determinations ($n = 9$). * $P < 0.0001$ as compared with vehicle treated control group as determined by one-way analysis of variance with Tukey's post hoc test.

that the chemotactic defects in AGS4/Gpsm3-null mice was primarily directional and not due to an overall increase in migratory capacity (Robichaux, W.G. III, Branham-O'Connor, M., and Blumer, J.B., unpublished observations). In addition, flow cytometry analysis revealed that chemokine receptor levels were unaltered in leukocytes from AGS4/Gpsm3-null mice, thus indicating that the chemotactic defects observed were not due to the loss of chemokine receptor expression (Hwang, I.-Y., Vural, A., and Kehrl, J., H., unpublished observations).

Gene expression databases indicate that AGS4 is highly expressed in neutrophils (Immunological Genome Project Database, 2014, www.immgen.org; Heng and Painter, 2008); indeed, we observed high levels of AGS4 expression in primary mouse neutrophils (Fig. 5A). Therefore, we measured chemotactic responses in primary neutrophils from WT and AGS4/Gpsm3-null mice and observed significant defects in AGS4/Gpsm3-null neutrophil chemotaxis to fMLP (Fig. 5B). Interestingly, the chemotactic defect observed was

dose-dependent, with a reduction of $\sim 60\%$ in directed migration to the highest dose of agonist (Fig. 5B), suggesting that AGS4/Gpsm3 may play a role in shaping cell responses at high levels of receptor activation. We next asked whether the requirement of AGS4/Gpsm3 for proper neutrophil chemotaxis *ex vivo* was also observed *in vivo*. As an initial approach to addressing this question, we used an induced peritonitis model by i.p. injection of thioglycollate to measure the recruitment of neutrophils to the site of inflammation. Whereas induced peritonitis resulted in a significant accumulation of WT neutrophils in the i.p. cavity, the level of AGS4/Gpsm3-null neutrophils recruited to the i.p. cavity was reduced by $\sim 80\%$ (Fig. 5C, left panel). Levels of neutrophils in the blood and bone marrow were not different in WT and AGS4/Gpsm3-null mice (Fig. 5C, center and right panels). These data suggest a possible deficiency in extravasation or a tardive response in AGS4/Gpsm3-null neutrophils.

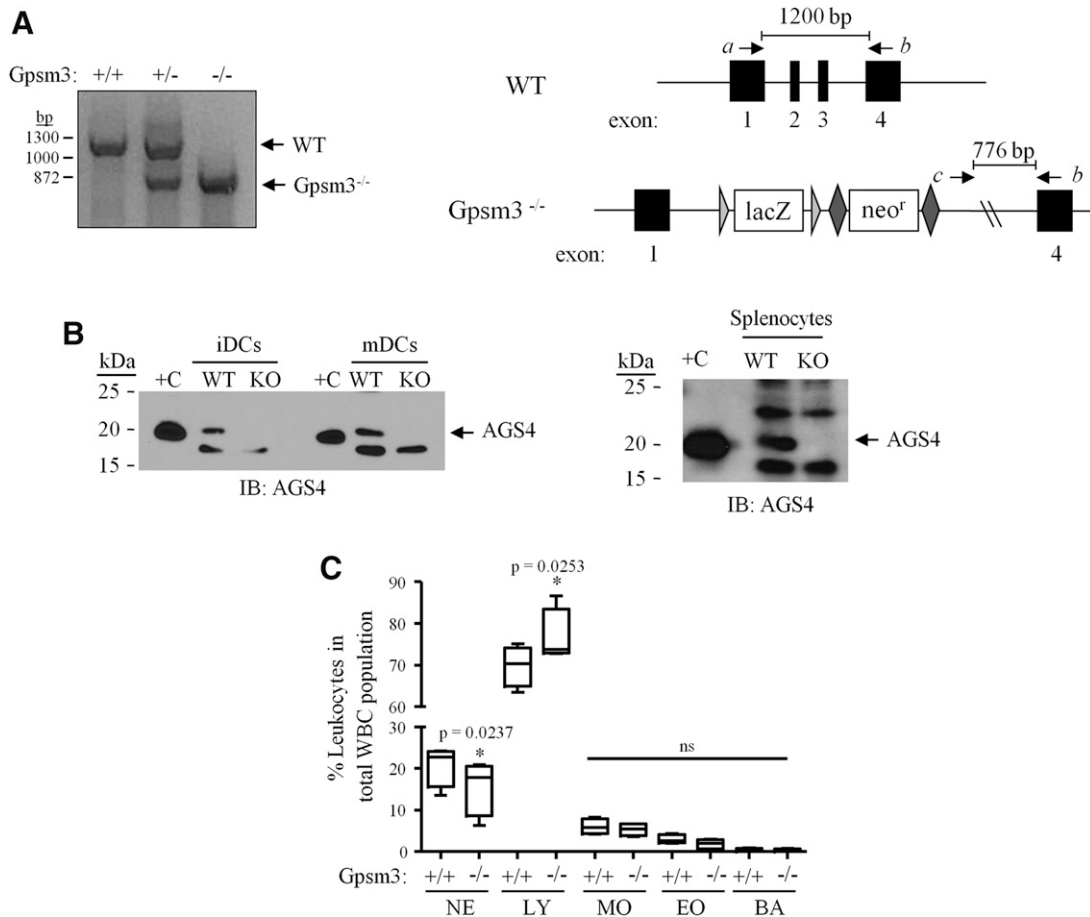


Fig. 2. Loss of AGS4 results in altered leukocyte population phenotype. (A) Left panel: A three-primer PCR approach was used to genotype AGS4/Gpsm3 wild-type (+/+), heterozygous (+/-) and null (-/-) mice. Right panel: Schematic depicting the strategy used to generate and polymerase chain reaction (PCR) genotype AGS4/Gpsm3-null mice as described in *Materials and Methods*. DNA primers *a*, *b*, and *c* (corresponding to “Gpsm3 16651 forward,” “Common 3’ forward” and “CSD-Gpsm3-SR1,” respectively; see *Materials and Methods* for additional details) were used in a three-primer PCR reaction in which a wild-type product at 1200 bp resulted from priming from primers *a* and *b*, and an AGS4/Gpsm3^{-/-} product at 776 bp resulted from priming from primers *b* and *c*. (B) Lysates (100 μ g/lane) from primary immature dendritic cells (iDCs), mature dendritic cells (mDCs) (left panel), and splenocytes (right panel) from WT (wild-type), and Gpsm3-null mice were subjected to SDS-PAGE, transferred to PVDF membranes, and immunoblotted (IB) with AGS4 antisera as described in *Materials and Methods*. “+C” refers to lysate prepared from HEK293 cells transfected with pcDNA3::AGS4 after 24 hours as described in *Materials and Methods*. (C) Complete blood count (CBC) analysis was from blood collected from WT and AGS4/Gpsm3-null mice as described in *Materials and Methods*. The percentage of leukocyte populations in relation to total number of white blood cells was calculated and compared between WT and AGS4/Gpsm3-null littermate pairs. BA, basophils; EO, eosinophils; LY, lymphocytes; MO, monocytes; NE, neutrophils. Data are represented as the mean \pm S.E. from four pairs of 12-week-old mice.

Discussion

A growing number of cellular and physiologic roles have been ascribed to GPR proteins in systems where signal modulation and adaptation are critical for system responsiveness (Bowers et al., 2004, 2008; Yao et al., 2005, 2006; Blumer et al., 2008; Nadella et al., 2010; Regner et al., 2011; Chauhan et al., 2012; Kwon et al., 2012; Giguère et al., 2013; Kamakura et al., 2013; Branham-O’Connor et al., 2014; Singh et al., 2014). The immune system is certainly an area rich in signaling modulation and adaptation and requires dynamic signal processing and spatially integrated G-protein signaling (Cho and Kehrl, 2009; Kehrl et al., 2009). Indeed, G proteins and accessory proteins, such as regulator of G-protein signaling (RGS) proteins, play critical roles in signal processing in the immune system (Rudolph et al., 1995; Huang et al., 2003; Han et al., 2005, 2006; Skokowa et al., 2005; Hwang et al., 2007; Pero et al., 2007; Zarbock et al., 2007; Cho and Kehrl, 2009; Kehrl et al., 2009; Cho et al., 2012; Wiege et al., 2012, 2013; Surve et al., 2014, 2016; Rangel-Moreno et al., 2016).

Alterations in circulating populations of neutrophils and lymphocytes in AGS4/Gpsm3-null mice may suggest a defect either in the production or differentiation of these cells or a defect in their egress from the bone marrow into the circulation. Interestingly, similar phenotypes including mild neutropenia and a defect in neutrophil migration were also observed in mice with an RGS-insensitive Gnai2 knock-in allele (Cho et al., 2012), suggesting that regulation of the duration of G-protein signaling subsequent to chemoattractant exposure is critical in neutrophil mobility and recruitment to sites of inflammation.

Our initial approach to investigating the role of AGS4 in chemokine signal processing reported in this manuscript used key prototype chemokine and chemoattractant receptors. AGS4 may possess selectivity for modulating G-protein signal processing for different chemokine receptors, and this is the basis for future studies. We have shown here that AGS4 forms a G α i-dependent complex with the chemokine receptor CXCR4 that is regulated by agonist (Fig. 1). Based on data

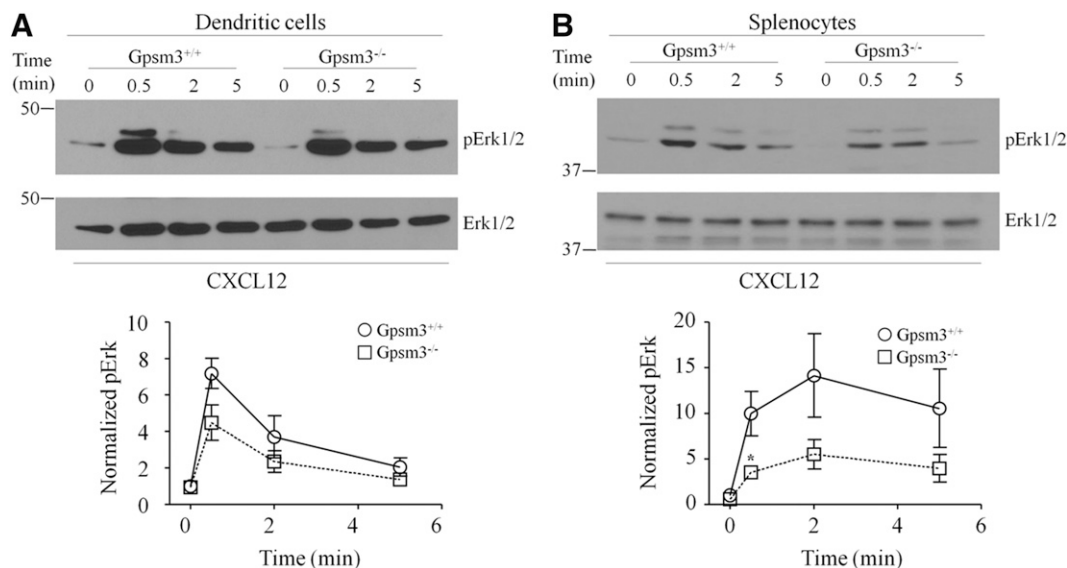


Fig. 3. AGS4-KO dendritic cells and splenocytes exhibit defects in CXCL12-stimulated phosphorylation of ERK1/2. Single-cell suspensions of WT and AGS4/Gpsm3-null cultured dendritic cells (A) or splenocytes (B) were treated with 200 ng/ml CXCL12 as described in *Materials and Methods*. At the indicated times, cells were lysed in 1% NP40 lysis buffer containing protease and phosphatase inhibitors, subjected to SDS-PAGE (50 μg/lane), transferred to PVDF, and immunoblotted with anti-phospho-Erk (Y204) and total Erk-specific antibodies. Representative immunoblots are shown in the upper panels, and densitometric analysis of at least three independent experiments (represented as means ± S.E.) are shown in the lower panels (**P* < 0.05).

presented here and elsewhere, this agonist regulation is likely due to the apparent coupling of the Gαi-AGS4 complex directly with the agonist-bound GPCR (Robichaux et al., 2015). Although our data indicate defective chemokine signal integration from CXCR4 activation upon loss of AGS4 expression in dendritic cells and lymphocytes, we cannot rule out a potential role for CXCR7, which can also bind CXCL12; however, CXCR7-mediated responses to CXCL12 are G-protein independent (Burns et al., 2006; Zabel et al., 2009;

Rajagopal et al., 2010), thus likely limiting the direct involvement of G-protein modulators like AGS4 in CXCL12/CXCR7-mediated signaling. There are also reports of potential CXCR4-CXCR7 dimerization (Levoye et al., 2009; Décaillot et al., 2011); thus, the interplay between these two receptors and the influence AGS4 may have on such a complex may be of future interest.

We previously demonstrated that the Gαi-GPR module can be regulated by a 7-TMR (Oner et al., 2010a,b; Robichaux

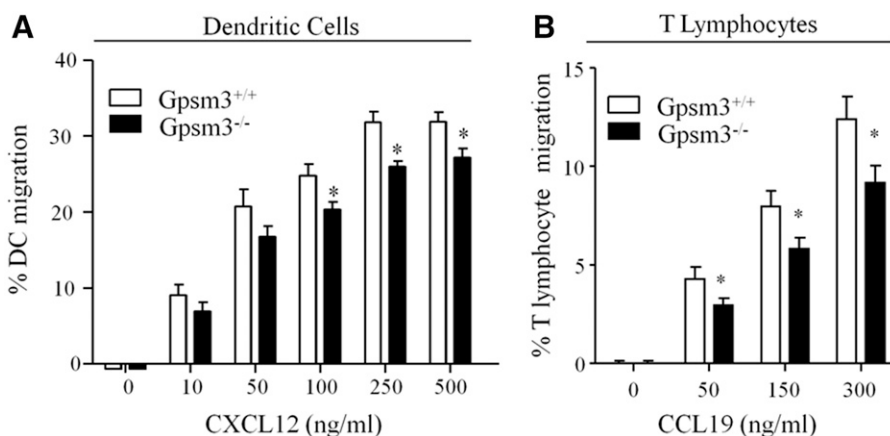


Fig. 4. Loss of AGS4 results in defective chemotaxis in primary leukocytes. (A) Bone marrow-derived dendritic cells (BMDCs) from WT and AGS4/Gpsm3-null mice were prepared as described in *Materials and Methods*. BMDCs were loaded in transwell migration chambers with the bottom chamber containing serum-free RPMI in the absence and presence of 10, 50, 100, 250, and 500 ng/ml CXCL12 as indicated. After 20 hours at 37°C, cells in the bottom chamber were counted, and the percentage of cells migrated was calculated relative to the input where the number of cells migrating to vehicle only was subtracted. Data are represented as the mean ± S.E. of a minimum four independent experiments with at least triplicate determinations (**P* < 0.01). (B) T lymphocytes were isolated from freshly harvested splenocytes of WT and AGS4/Gpsm3-null mice after red blood cell lysis and filtering to remove cell and tissue aggregates as described in *Materials and Methods*. Cells were loaded in transwell migration chambers with bottom chambers containing serum-free RPMI in the absence or presence of 50, 150, and 300 ng/ml CCL19. After 5 hours at 37°C, cells in the bottom chamber were counted, and the percentage of cells migrated was calculated relative to the input where the number of cells migrating to vehicle only was subtracted. Data are represented as the mean ± S.E. of at a minimum of four independent experiments with at least triplicate determinations (**P* < 0.01).

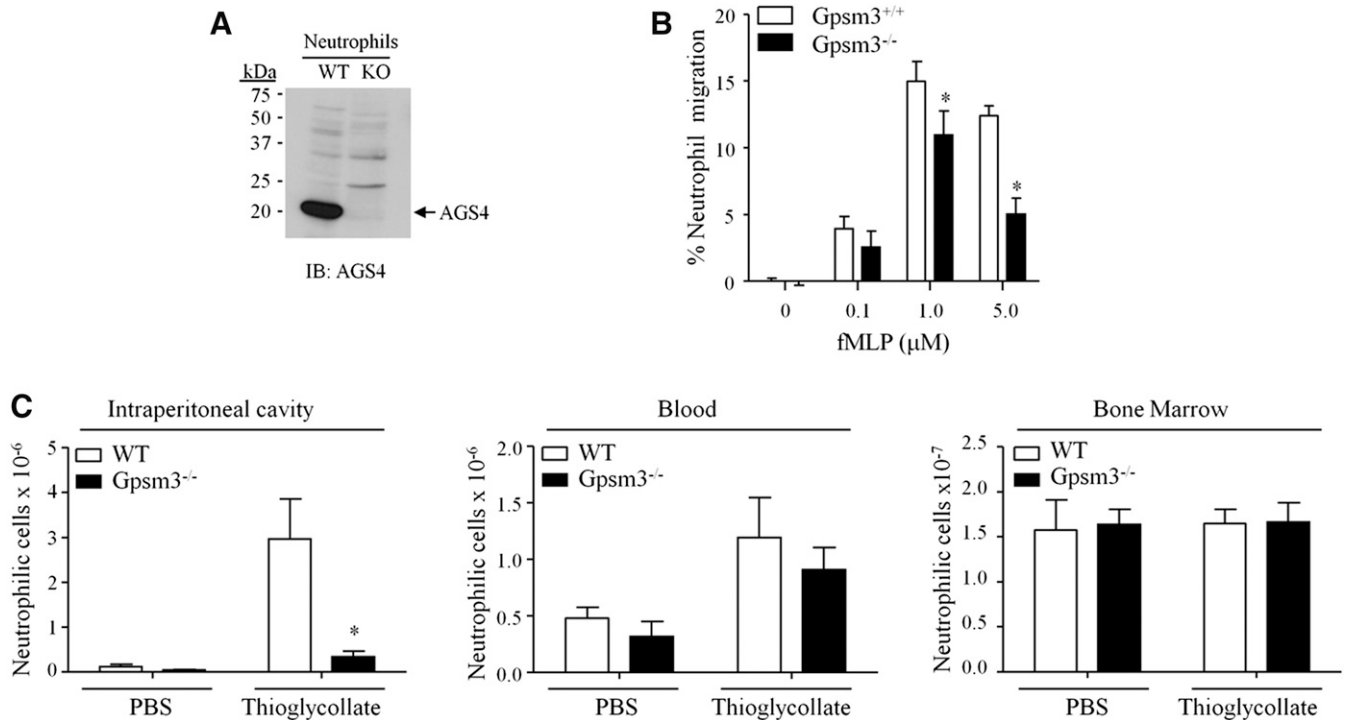


Fig. 5. AGS4-KO neutrophils demonstrate reduced migration to site of inflammation. (A,B) Neutrophils were isolated from freshly harvested bone marrow from WT and AGS4/Gpsm3-null mice using Percoll gradient centrifugation as described in *Materials and Methods*. (A) Neutrophil lysates (100 μ g) were prepared with 1% NP-40 lysis buffer and subjected to SDS-PAGE, transferred to PVDF, and immunoblotted with AGS4 antisera as described in *Materials and Methods*. The representative immunoblot shown is reflective of at least three independent experiments. (B) Isolated neutrophils were loaded in transwell migration chambers with the bottom chamber containing serum-free RPMI in the absence and presence of 0.1, 1.0, and 5.0 μ M fMLP. After 3 hours at 37°C, cells in the bottom chamber were counted, and the percentage of cells migrated was calculated relative to the input where the number of cells migrating to vehicle only was subtracted. (C) WT and AGS4/Gpsm3-null mice received 1 ml of i.p. injections of 4% thioglycollate or sterile PBS to induce localized inflammation as described in *Materials and Methods*. Two hours postinjection, mice were euthanized and the i.p. cavity was lavaged with 10 ml of cold, sterile PBS (left panel). Blood (middle panel) was collected by cardiac stick, and femurs were processed to harvest bone marrow cells (right panel) as described in *Materials and Methods*. Red blood cells were lysed from cell preparations, and the remaining cells were stained with CD11b-FITC and Ly6G-PE for flow cytometry analysis of neutrophil numbers in each tissue. Neutrophil cell numbers were calculated using total events collected, applying flow rate and percentage of dual positive cells, followed by dilutions carried out during processing of the cells. Data are represented as the mean \pm S.E. of $n = 4$ mice per genotype. * $P < 0.05$.

et al., 2015). Recently, we reported that this regulation reflects a direct engagement of G α i-GPR with the 7-TMR analogous to canonical G α β γ . It is possible that direct input from chemoattractant receptors to the G α i-AGS4 module may play an important modulatory role in chemokine signal processing, and the loss of this alternative mode of signal input to G α i signaling may be responsible for the defects observed in AGS4/Gpsm3-null leukocytes. Such regulation would be a novel mechanism for G-protein signal processing, as G α i-specific roles in chemoattractant signal processing have been elusive; however, some reports have suggested G α i-specific functions in leukocyte responses to chemokines (Surve et al., 2016). Whereas G β γ is generally considered the primary G-protein signaling unit within leukocytes (Arai et al., 1997; Neptune and Bourne, 1997; Peracino et al., 1998; Lehmann et al., 2008; Zhang et al., 2010) (e.g., elevations in intracellular Ca²⁺, activation of PI3K γ and downstream activation of small GTPases required for directed migration) Surve et al. (2016) reported that G α i signaling in leukocytes appears to be required to locally counteract G β γ -mediated increases in cAMP to facilitate cell polarity and directed migration. We speculate that the G α i-AGS4 module, and perhaps G α i-AGS3 complexes as well (Blumer and Lanier, 2014; Branham-O'Connor et al., 2014; Robichaux et al., 2015), by coupling directly with chemokine receptors, may increase the available

pool of G α i-GTP to assist in dampening local cAMP levels to facilitate leukocyte polarity and directed migration.

Within the immune system, AGS4 is highly expressed in neutrophils (Fig. 5), perhaps higher than any other immune cell type (www.immgen.org; Heng and Painter, 2008), which suggests an important role for AGS4 in neutrophils and also provides an attractive model for studying the role of AGS4 in the innate immune system. The apparent dose-dependent chemotactic defect observed in AGS4/Gpsm3-null neutrophils (Fig. 5B) suggests that AGS4 may play an important role in modulating cellular responses at higher levels of receptor activation. Similar observations were noted for regulator of G-protein signaling 1 (RGS1), another accessory protein important for chemokine-regulated G-protein signal processing (Han et al., 2006; Hwang et al., 2010). Furthermore, our data indicate that AGS4-null neutrophils have a defect in chemoattractant-mediated migration *ex vivo*, which manifests in a defect in neutrophil recruitment to sites of inflammation *in vivo* (Fig. 5). It is interesting to note that either inhibition or loss of G α i₂ expression in leukocytes and endothelial cells also impairs neutrophil extravasation to sites of inflammation (Warnock et al., 1998; Pero et al., 2007; Zarbock et al., 2007; Wiege et al., 2012). Thus, aberrant transmigration of AGS4/Gpsm3-null neutrophils from the blood to the i.p. cavity may reflect simultaneous aberrant

Gai₂ signaling in both neutrophils and endothelial cells, which together contribute to the observed defects in innate immunity. Future studies are aimed at validating these results in primary human leukocytes. Taken together, these data suggest that AGS4 may play a role in the inflammatory response and that the AGS4-Gai module may be an attractive target for the development of potential therapeutics.

Acknowledgments

The authors thank Ellen Maher, Christine Webster, and Hunter Matthews for expert technical assistance; Dr. Michel Bouvier (University of Montreal, Montreal, ON, CA) for providing CXCR4 and CXCR4-Venus expression plasmids; and Dr. Stephen Lanier (Wayne State University) for helpful discussions and support.

Authorship Contributions

Participated in research design: Robichaux, Branham-O'Connor, Hwang, Vural, Kehrl, Blumer.

Conducted experiments: Robichaux, Branham-O'Connor, Hwang, Vural, Kehrl, Blumer.

Contributed new reagents or analytic tools: Robichaux, Branham-O'Connor, Hwang, Vural, Kehrl, Blumer.

Performed data analysis: Robichaux, Branham-O'Connor, Hwang, Vural, Kehrl, Blumer.

Wrote or contributed to the writing of the manuscript: Robichaux, Branham-O'Connor, Vural, Kehrl, Blumer.

References

- Ahn R, Ding YC, Murray J, Fasano A, Green PH, Neuhausen SL, and Garner C (2012) Association analysis of the extended MHC region in celiac disease implicates multiple independent susceptibility loci. *PLoS One* **7**:e36926.
- Arai H, Tsou CL, and Charo IF (1997) Chemotaxis in a lymphocyte cell line transfected with C-C chemokine receptor 2B: evidence that directed migration is mediated by betagamma dimers released by activation of Galphai-coupled receptors. *Proc Natl Acad Sci USA* **94**:14495–14499.
- Basu S and Broxmeyer HE (2005) Transforming growth factor-beta1 modulates responses of CD34+ cord blood cells to stromal cell-derived factor-1/CXCL12. *Blood* **106**:485–493.
- Basu S and Broxmeyer HE (2009) CCR5 ligands modulate CXCL12-induced chemotaxis, adhesion, and Akt phosphorylation of human cord blood CD34+ cells. *J Immunol* **183**:7478–7488.
- Billard MJ, Gall BJ, Richards KL, Siderovski DP, and Tarrant TK (2014) G protein signaling modulator-3: a leukocyte regulator of inflammation in health and disease. *Am J Clin Exp Immunol* **3**:97–106.
- Blumer JB, Chandler LJ, and Lanier SM (2002) Expression analysis and subcellular distribution of the two G-protein regulators AGS3 and LGN indicate distinct functionality: localization of LGN to the midbody during cytokinesis. *J Biol Chem* **277**:15897–15903.
- Blumer JB and Lanier SM (2014) Activators of G protein signaling exhibit broad functionality and define a distinct core signaling triad. *Mol Pharmacol* **85**:388–396.
- Blumer JB, Lord K, Saunders TL, Pacchioni A, Black C, Lazartigues E, Varner KJ, Gettys TW, and Lanier SM (2008) Activator of G protein signaling 3 null mice: I. Unexpected alterations in metabolic and cardiovascular function. *Endocrinology* **149**:3842–3849.
- Boudot A, Kerdivel G, Lecomte S, Flouriot G, Desille M, Godey F, Leveque J, Tas P, Le Dréan Y, and Pakdel F (2014) COUP-TFI modifies CXCL12 and CXCR4 expression by activating EGF signaling and stimulates breast cancer cell migration. *BMC Cancer* **14**:407.
- Boullaran C, Hwang IY, Kamenyeva O, Park C, Harrison K, Huang Z, and Kehrl JH (2015) B lymphocyte-specific loss of Ric-8A results in a Gα protein deficit and severe humoral immunodeficiency. *J Immunol* **195**:2090–2102.
- Boullaran C and Kehrl JH (2014) Implications of non-canonical G-protein signaling for the immune system. *Cell Signal* **26**:1269–1282.
- Bowers MS, Hopf FW, Chou JK, Guillory AM, Chang SJ, Janak PH, Bonci A, and Diamond I (2008) Nucleus accumbens AGS3 expression drives ethanol seeking through G betagamma. *Proc Natl Acad Sci USA* **105**:12533–12538.
- Bowers MS, McFarland K, Lake RW, Peterson YK, Lapish CC, Gregory ML, Lanier SM, and Kalivas PW (2004) Activator of G protein signaling 3: a gatekeeper of cocaine sensitization and drug seeking. *Neuron* **42**:269–281.
- Branham-O'Connor M, Robichaux WG, 3rd, Zhang XK, Cho H, Kehrl JH, Lanier SM, and Blumer JB (2014) Defective chemokine signal integration in leukocytes lacking activator of G protein signaling 3 (AGS3). *J Biol Chem* **289**:10738–10747.
- Burns JM, Summers BC, Wang Y, Melikian A, Berahovich R, Miao Z, Penfold ME, Sunshine MJ, Littman DR, Kuo CJ, et al. (2006) A novel chemokine receptor for SDF-1 and I-TAC involved in cell survival, cell adhesion, and tumor development. *J Exp Med* **203**:2201–2213.
- Cao X, Cismowski MJ, Sato M, Blumer JB, and Lanier SM (2004) Identification and characterization of AGS4: a protein containing three G-protein regulatory motifs that regulate the activation state of Gα_i. *J Biol Chem* **279**:27567–27574.

- Chauhan S, Jelen F, Sharina I, and Martin E (2012) The G-protein regulator LGN modulates the activity of the NO receptor soluble guanylate cyclase. *Biochem J* **446**:445–453.
- Cho H, Kamenyeva O, Yung S, Gao JL, Hwang IY, Park C, Murphy PM, Neubig RR, and Kehrl JH (2012) The loss of RGS protein-Gα_{i2} interactions results in markedly impaired mouse neutrophil trafficking to inflammatory sites. *Mol Cell Biol* **32**:4561–4571.
- Cho H and Kehrl JH (2009) Regulation of immune function by G protein-coupled receptors, trimeric G proteins, and RGS proteins. *Prog Mol Biol Transl Sci* **86**:249–298.
- Cismowski MJ, Takesono A, Ma C, Lizano JS, Xie X, Fuernkrantz H, Lanier SM, and Duzic E (1999) Genetic screens in yeast to identify mammalian nonreceptor modulators of G-protein signaling. *Nat Biotechnol* **17**:878–883.
- Décaillot FM, Kazmi MA, Lin Y, Ray-Saha S, Sakmar TP, and Sachdev P (2011) CXCR7/CXCR4 heterodimer constitutively recruits beta-arrestin to enhance cell migration. *J Biol Chem* **286**:32188–32197.
- Delgado-Martín C, Escribano C, Pablos JL, Riol-Blanco L, and Rodríguez-Fernández JL (2011) Chemokine CXCL12 uses CXCR4 and a signaling core formed by bi-functional Akt, extracellular signal-regulated kinase (ERK)1/2, and mammalian target of rapamycin complex 1 (mTORC1) proteins to control chemotaxis and survival simultaneously in mature dendritic cells. *J Biol Chem* **286**:37222–37236.
- Dorner BG, Dorner MB, Zhou X, Opitz C, Mora A, Güttler S, Hutloff A, Mages HW, Ranke K, Schaefer M, et al. (2009) Selective expression of the chemokine receptor XCR1 on cross-presenting dendritic cells determines cooperation with CD8+ T cells. *Immunity* **31**:823–833.
- Gall BJ, Schroer AB, Gross JD, Setola V, and Siderovski DP (2016) Reduction of GPM3 expression akin to the arthritis-protective SNP rs204989 differentially affects migration in a neutrophil model. *Genes Immun* **17**:321–327.
- Giguère PM, Billard MJ, Laroche G, Buckley BK, Timoshchenko RG, McGinnis MW, Esserman D, Foreman O, Liu P, Siderovski DP, et al. (2013) G-protein signaling modulator-3, a gene linked to autoimmune diseases, regulates monocyte function and its deficiency protects from inflammatory arthritis. *Mol Immunol* **54**:193–198.
- Giguère PM, Gall BJ, Ezekwe EA, Jr., Laroche G, Buckley BK, Kebeier C, Wilson JE, Ting JP, Siderovski DP, and Dunca JA (2014) G Protein signaling modulator-3 inhibits the inflammasome activity of NLRP3. *J Biol Chem* **289**:33245–33257.
- Hamdan FF, Percherancier Y, Breton B, and Bouvier M (2006) Monitoring protein-protein interactions in living cells by bioluminescence resonance energy transfer (BRET). *Curr Protoc Neurosci* **5**:23 DOI: 10.1002/0471142301.n50523s34.
- Han JI, Huang NN, Kim DU, and Kehrl JH (2006) RGS1 and RGS13 mRNA silencing in a human B lymphoma line enhances responsiveness to chemoattractants and impairs desensitization. *J Leukoc Biol* **79**:1357–1368.
- Han SB, Moratz C, Huang NN, Kelsall B, Cho H, Shi CS, Schwartz O, and Kehrl JH (2005) Rgs1 and Gnai2 regulate the entrance of B lymphocytes into lymph nodes and B cell motility within lymph node follicles. *Immunity* **22**:343–354.
- Heng TS and Painter MW; Immunological Genome Project Consortium (2008) The Immunological Genome Project: networks of gene expression in immune cells. *Nat Immunol* **9**:1091–1094.
- Huang NN, Becker S, Boullaran C, Kamenyeva O, Vural A, Hwang IY, Shi CS, and Kehrl JH (2014) Canonical and noncanonical g-protein signaling helps coordinate actin dynamics to promote macrophage phagocytosis of zymosan. *Mol Cell Biol* **34**:4186–4199.
- Huang TT, Zong Y, Dalwadi H, Chung C, Miceli MC, Spicher K, Birnbaumer L, Braun J, and Aranda R (2003) TCR-mediated hyper-responsiveness of autoimmune Galphai2(-/-) mice is an intrinsic naive CD4(+) T cell disorder selective for the Galphai2 subunit. *Int Immunol* **15**:1359–1367.
- Hwang IY, Hwang KS, Park C, Harrison KA, and Kehrl JH (2013) Rgs13 constrains early B cell responses and limits germinal center sizes. *PLoS One* **8**:e61039.
- Hwang IY, Park C, Harrison KA, Huang NN, and Kehrl JH (2010) Variations in Gnai2 and Rgs1 expression affect chemokine receptor signaling and the organization of secondary lymphoid organs. *Genes Immun* **11**:384–396.
- Hwang IY, Park C, Harrison K, Boullaran C, Galés C, and Kehrl JH (2015) An essential role for RGS protein/Goi2 interactions in B lymphocyte-directed cell migration and trafficking. *J Immunol* **194**:2128–2139.
- Hwang IY, Park C, and Kehrl JH (2007) Impaired trafficking of Gnai2+/- and Gnai2-/- T lymphocytes: implications for T cell movement within lymph nodes. *J Immunol* **179**:439–448.
- Kamakura S, Nomura M, Hayase J, Iwakiri Y, Nishikimi A, Takayanagi R, Fukui Y, and Sumimoto H (2013) The cell polarity protein mInsc regulates neutrophil chemotaxis via a noncanonical G protein signaling pathway. *Dev Cell* **26**:292–302.
- Kehrl JH, Hwang IY, and Park C (2009) Chemoattractant receptor signaling and its role in lymphocyte motility and trafficking. *Curr Top Microbiol Immunol* **334**:107–127.
- Kiliszek M, Burzynska B, Michalak M, Gora M, Winkler A, Maciejak A, Leszczynska A, Gajda E, Kochanowski J, and Opolski G (2012) Altered gene expression pattern in peripheral blood mononuclear cells in patients with acute myocardial infarction. *PLoS One* **7**:e50054.
- Kimple RJ, Willard FS, Hains MD, Jones MB, Nweke GK, and Siderovski DP (2004) Guanine nucleotide dissociation inhibitor activity of the triple GoLoco motif protein G18: alanine-to-aspartate mutation restores function to an inactive second GoLoco motif. *Biochem J* **378**:801–808.
- Kupfer DM, White VL, Strayer DL, Crouch DJ, and Burian D (2013) Microarray characterization of gene expression changes in blood during acute ethanol exposure. *BMC Med Genomics* **6**:26.
- Kwon M, Pavlov TS, Nozu K, Rasmussen SA, Ilatovskaya DV, Lerch-Gaggl A, North LM, Kim H, Qian F, Sweeney WE, Jr, et al. (2012) G-protein signaling modulator 1 deficiency accelerates cystic disease in an orthologous mouse model of autosomal dominant polycystic kidney disease. *Proc Natl Acad Sci USA* **109**:21462–21467.
- Lehmann DM, Seneviratne AM, and Smrcka AV (2008) Small molecule disruption of G protein beta gamma subunit signaling inhibits neutrophil chemotaxis and inflammation. *Mol Pharmacol* **73**:410–418.
- Levoe A, Balabanian K, Baleux F, Bachelier F, and Lagane B (2009) CXCR7 heterodimerizes with CXCR4 and regulates CXCL12-mediated G protein signaling. *Blood* **113**:6085–6093.

- Moratz C, Hayman JR, Gu H, and Kehr JH (2004) Abnormal B-cell responses to chemokines, disturbed plasma cell localization, and distorted immune tissue architecture in *Rgs1*^{-/-} mice. *Mol Cell Biol* **24**:5767–5775.
- Moratz C, Kang VH, Druey KM, Shi CS, Scheschonka A, Murphy PM, Kozasa T, and Kehr JH (2000) Regulator of G protein signaling 1 (RGS1) markedly impairs Gi alpha signaling responses of B lymphocytes. *J Immunol* **164**:1829–1838.
- Nadella R, Blumer JB, Jia G, Kwon M, Akbulut T, Qian F, Sedlic F, Wakatsuki T, Sweeney WE, Jr, Wilson PD, et al. (2010) Activator of G protein signaling 3 promotes epithelial cell proliferation in PKD. *J Am Soc Nephrol* **21**:1275–1280.
- Nakou M, Knowlton N, Frank MB, Bertsias G, Osban J, Sandel CE, Papadaki H, Raptopoulou A, Sidiropoulos P, Kritikos I, et al. (2008) Gene expression in systemic lupus erythematosus: bone marrow analysis differentiates active from inactive disease and reveals apoptosis and granulopoiesis signatures. *Arthritis Rheum* **58**: 3541–3549.
- Neptune ER and Bourne HR (1997) Receptors induce chemotaxis by releasing the betagamma subunit of Gi, not by activating Gq or Gs. *Proc Natl Acad Sci USA* **94**: 14489–14494.
- Oner SS, An N, Vural A, Breton B, Bouvier M, Blumer JB, and Lanier SM (2010a) Regulation of the AGS3-Galphi signaling complex by a seven-transmembrane span receptor. *J Biol Chem* **285**:33949–33958.
- Oner SS, Blumer JB, and Lanier SM (2013) Group II activators of G-protein signaling: monitoring the interaction of G α with the G-protein regulatory motif in the intact cell. *Methods Enzymol* **522**:153–167.
- Oner SS, Maher EM, Breton B, Bouvier M, and Blumer JB (2010b) Receptor-regulated interaction of activator of G-protein signaling-4 and Galphi. *J Biol Chem* **285**:20588–20594.
- Peracino B, Borleis J, Jin T, Westphal M, Schwartz JM, Wu L, Bracco E, Gerisch G, Devreotes P, and Bozzaro S (1998) G protein beta subunit-null mutants are impaired in phagocytosis and chemotaxis due to inappropriate regulation of the actin cytoskeleton. *J Cell Biol* **141**:1529–1537.
- Pero RS, Borchers MT, Spicher K, Ochkur SI, Sikora L, Rao SP, Abdala-Valencia H, O'Neill KR, Shen H, McGarry MP, et al. (2007) Galphi2-mediated signaling events in the endothelium are involved in controlling leukocyte extravasation. *Proc Natl Acad Sci USA* **104**:4371–4376.
- Petit I, Goichberg P, Spiegel A, Peled A, Brodie C, Seger R, Nagler A, Alon R, and Lapidot T (2005) Atypical PKC-zeta regulates SDF-1-mediated migration and development of human CD34⁺ progenitor cells. *J Clin Invest* **115**:168–176.
- Rajagopal S, Kim J, Ahn S, Craig S, Lam CM, Gerard NP, Gerard C, and Lefkowitz RJ (2010) Beta-arrestin- but not G protein-mediated signaling by the “decoy” receptor CXCR7. *Proc Natl Acad Sci USA* **107**:628–632.
- Rangel-Moreno J, To JY, Owen T, Goldman BI, Smrcka AV, and Anolik JH (2016) Inhibition of G protein $\beta\gamma$ subunit signaling abrogates nephritis in lupus-prone mice. *Arthritis Rheumatol* **68**:2244–2256.
- Regner KR, Nozu K, Lanier SM, Blumer JB, Avner ED, Sweeney WE, Jr, and Park F (2011) Loss of activator of G-protein signaling 3 impairs renal tubular regeneration following acute kidney injury in rodents. *FASEB J* **25**:1844–1855.
- Robichaux WG III, Oner SS, Lanier SM, and Blumer JB (2015) Direct coupling of a seven-transmembrane-span receptor to a Gai G-protein regulatory motif complex. *Mol Pharmacol* **88**:231–237.
- Rudolph U, Finegold MJ, Rich SS, Harriman GR, Srinivasan Y, Brabet P, Boulay G, Bradley A, and Birnbaumer L (1995) Ulcerative colitis and adenocarcinoma of the colon in G alpha i2-deficient mice. *Nat Genet* **10**:143–150.
- Sagar D, Lamontagne A, Foss CA, Khan ZK, Pomper MG, and Jain P (2012) Dendritic cell CNS recruitment correlates with disease severity in EAE via CCL2 chemotaxis at the blood-brain barrier through paracellular transmigration and ERK activation. *J Neuroinflammation* **9**:245.
- Schmidt N, Art J, Forsch I, Werner A, Erkel G, Jung M, Horke S, Kleinert H, and Pautz A (2012) The anti-inflammatory fungal compound (S)-curvularin reduces proinflammatory gene expression in an in vivo model of rheumatoid arthritis. *J Pharmacol Exp Ther* **343**:106–114.
- Singh V, Raghuvanshi SK, Smith N, Rivers EJ, and Richardson RM (2014) G protein-coupled receptor kinase-6 interacts with activator of G protein signaling-3 to regulate CXCR2-mediated cellular functions. *J Immunol* **192**:2186–2194.
- Skokowa J, Ali SR, Felda O, Kumar V, Konrad S, Shushakova N, Schmidt RE, Piekorz RP, Nürnberg B, Spicher K, et al. (2005) Macrophages induce the inflammatory response in the pulmonary Arthus reaction through G alpha i2 activation that controls C5aR and Fc receptor cooperation. *J Immunol* **174**: 3041–3050.
- Surve CR, Lehmann D, and Smrcka AV (2014) A chemical biology approach demonstrates G protein $\beta\gamma$ subunits are sufficient to mediate directional neutrophil chemotaxis. *J Biol Chem* **289**:17791–17801.
- Surve CR, To JY, Malik S, Kim M, and Smrcka AV (2016) Dynamic regulation of neutrophil polarity and migration by the heterotrimeric G protein subunits Gai-GTP and G $\beta\gamma$. *Sci Signal* **9**:ra22.
- Takesono A, Cismowski MJ, Ribas C, Bernard M, Chung P, Hazard S III, Duzic E, and Lanier SM (1999) Receptor-independent activators of heterotrimeric G-protein signaling pathways. *J Biol Chem* **274**:33202–33205.
- Tilton B, Ho L, Oberlin E, Loetscher P, Baleux F, Clark-Lewis I, and Thelen M (2000) Signal transduction by CXC chemokine receptor 4. Stromal cell-derived factor 1 stimulates prolonged protein kinase B and extracellular signal-regulated kinase 2 activation in T lymphocytes. *J Exp Med* **192**:313–324.
- Vural A, Al-Khodor S, Cheung GY, Shi CS, Srinivasan L, McQuiston TJ, Hwang IY, Yeh AJ, Blumer JB, Briken V, et al. (2016) Activator of G-protein signaling 3-induced lysosomal biogenesis limits macrophage intracellular bacterial infection. *J Immunol* **196**:846–856.
- Warnock RA, Askari S, Butcher EC, and von Andrian UH (1998) Molecular mechanisms of lymphocyte homing to peripheral lymph nodes. *J Exp Med* **187**: 205–216.
- Wiege K, Ali SR, Gewecke B, Novakovic A, Konrad FM, Pexa K, Beer-Hammer S, Reutershan J, Piekorz RP, Schmidt RE, et al. (2013) Gai2 is the essential Gai protein in immune complex-induced lung disease. *J Immunol* **190**:324–333.
- Wiege K, Le DD, Syed SN, Ali SR, Novakovic A, Beer-Hammer S, Piekorz RP, Schmidt RE, Nürnberg B, and Gessner JE (2012) Defective macrophage migration in Gai2- but not Gai3-deficient mice. *J Immunol* **189**:980–987.
- Yan C, Ding X, Dasgupta N, Wu L, and Du H (2012) Gene profile of myeloid-derived suppressive cells from the bone marrow of lysosomal acid lipase knock-out mice. *PLoS One* **7**:e30701.
- Yao L, McFarland K, Fan P, Jiang Z, Inoue Y, and Diamond I (2005) Activator of G protein signaling 3 regulates opiate activation of protein kinase A signaling and relapse of heroin-seeking behavior. *Proc Natl Acad Sci USA* **102**:8746–8751.
- Yao L, McFarland K, Fan P, Jiang Z, Ueda T, and Diamond I (2006) Adenosine A2a blockade prevents synergy between mu-opiate and cannabinoid CB1 receptors and eliminates heroin-seeking behavior in addicted rats. *Proc Natl Acad Sci USA* **103**: 7877–7882.
- Zabel BA, Wang Y, Lewén S, Berahovich RD, Penfold ME, Zhang P, Powers J, Summers BC, Miao Z, Zhao B, et al. (2009) Elucidation of CXCR7-mediated signaling events and inhibition of CXCR4-mediated tumor cell transendothelial migration by CXCR7 ligands. *J Immunol* **183**:3204–3211.
- Zarbock A, Deem TL, Burcin TL, and Ley K (2007) Galphi2 is required for chemokine-induced neutrophil arrest. *Blood* **110**:3773–3779.
- Zhang Y, Tang W, Jones MC, Xu W, Halene S, and Wu D (2010) Different roles of G protein subunits beta1 and beta2 in neutrophil function revealed by gene expression silencing in primary mouse neutrophils. *J Biol Chem* **285**: 24805–24814.
- Zhao P, Nguyen CH, and Chidiac P (2010) The proline-rich N-terminal domain of G18 exhibits a novel G protein regulatory function. *J Biol Chem* **285**:9008–9017.
- Zhong J, Kim MS, Chaerkady R, Wu X, Huang TC, Getnet D, Mitchell CJ, Palapetta SM, Sharma J, O'Meally RN, et al. (2012) TSLP signaling network revealed by SILAC-based phosphoproteomics. *Mol Cell Proteomics* **11**:M112 017764.

Address correspondence to: Joe B. Blumer, Department of Cell and Molecular Pharmacology and Experimental Therapeutics, Medical University of South Carolina, 173 Ashley Ave, BSB358, MSC509, Charleston, SC 29425. E-mail: blumerjb@musc.edu